

# Photoproduction of single inclusive jets at future $ep$ colliders in next-to-leading order QCD

B. Jäger

*KEK Theory Division, Tsukuba 305-0801, Japan*

## Abstract

A next-to-leading order QCD calculation for single-inclusive jet photoproduction in unpolarized and longitudinally polarized lepton-hadron collisions is presented which consistently includes “direct” and “resolved” photon contributions. The computation is performed within the “small-cone approximation” in a largely analytical form. Phenomenological aspects of jet production at future  $ep$  colliders such as the CERN-LHeC and the polarized BNL-eRHIC are discussed, placing particular emphasis on the perturbative stability of the predictions and the possibility to constrain the parton content of the photon.

PACS numbers: 12.38.Bx,13.60.Hb,13.88+e

## I. INTRODUCTION

Recent years have seen encouraging progress in the understanding of the inner structure of hadrons, triggered by precision measurements at high energy colliders, in particular the DESY-HERA. The knowledge gained on the dynamics which governs the interaction of color-charged particles is crucial as new experiments are probing even higher energies. The ultimate goal of the upcoming CERN-LHC, for instance, is the verification of the standard model by the discovery of a light Higgs boson or, else, the identification of new physics not anticipated within this framework. Subsequent measurements at a future linear collider will constrain the parameters of the scenario realized in nature with even higher accuracy. However, poorly understood QCD effects may render the interpretation of new signatures in terms of physics beyond the standard model difficult. The precise determination of the parton densities entering the description of any hadronic reaction is thus more timely than ever.

Indeed, many improvements have been made recently on the parameterization of the proton distribution functions [1, 2, 3]. Much less is known about the hadronic structure of the photon. This ignorance severely limits the predictive power of photon-induced reactions since the *resolved* contributions, which are associated with its hadronic constituents, may be large at collider energies. As particularly promising means to cure this deficiency, jet-production processes in the photoproduction regime of lepton-hadron colliders, where the lepton beam acts as source of quasi-real photons, have been identified due to large production rates and small systematic uncertainties. The capability of HERA to constrain the partonic structure of the photon as well as the proton had been explored in great detail [4] and several NLO-QCD calculations for jet-photoproduction processes have become available, which turned out to describe data reasonably well [5, 6]. For a polarization upgrade of HERA, which has been discussed for some time [7], a thorough sensitivity study has been performed in Ref. [8]. Polarized predictions at NLO-QCD accuracy have been presented in [9] in the form of a flexible Monte-Carlo program.

Should single inclusive jets be used in the context of a “global analysis” including photoproduction data, however, fast codes are essential which are based on analytical methods. The aim of this work is thus to present a calculation of single-inclusive jet photoproduction in the framework of the “small-cone approximation” [10], which allows for an entirely ana-

lytical computation of partonic hard-scattering cross sections and has been demonstrated to approximate full jet cross sections extremely well in related  $pp$ -scattering reactions [11, 12].

Predictions can then be made for photoproduction cross sections at future lepton-proton colliders such as the planned BNL-eRHIC [13] and the CERN-LHeC [14] which is currently under scrutiny. In principle, the code developed also allows for the computation of jet-production observables at HERA. We refrain from presenting results for the HERA kinematics here, however, since a vast number of NLO-QCD studies for this setting is available in the literature [5, 6, 9].

The plan of the article is as follows: In Sec. II the technical framework used will be specified. Section III contains numerical results for single-inclusive jet production at the LHeC and the eRHIC, respectively. Conclusions will be given in Sec. IV.

## II. TECHNICAL FRAMEWORK

We consider single-inclusive jet photoproduction in unpolarized and in longitudinally polarized lepton-proton collisions at NLO-QCD accuracy, i.e., the reaction  $\ell p \rightarrow \ell' \text{jet} X$ . Provided the transverse momentum  $p_T$  of the jet is large, a polarized differential single-inclusive jet cross section can be written as a convolution

$$\begin{aligned}
 d\Delta\sigma^{\ell p} &\equiv \frac{1}{2} [d\sigma_{++} - d\sigma_{+-}] \\
 &= \sum_{a,b} \int dx_a dx_b \Delta f_a^\ell(x_a, \mu_f) \Delta f_b^p(x_b, \mu_f) \\
 &\times d\Delta\hat{\sigma}_{ab \rightarrow \text{jet} X}(S, x_a, x_b, \mu_r, \mu_f), \tag{1}
 \end{aligned}$$

where the subscripts “++” and “+-” refer to the helicities of the colliding leptons and protons, and  $S$  is the available c.m.s. energy squared. In Eq. (1),  $x_b$  denotes the momentum fraction of the proton which is taken by parton  $b$  and the  $\Delta f_b^p(x_b, \mu_f)$  are the longitudinally polarized parton distributions of the proton evaluated at a scale  $\mu_f$ . The summation in Eq. (1) is performed over all partonic channels  $a + b \rightarrow \text{jet} + X$  contributing to the reaction  $\ell p \rightarrow \ell' \text{jet} X$  with the corresponding spin-dependent cross sections  $d\Delta\hat{\sigma}_{ab \rightarrow \text{jet} X}$ , which are computed at NLO-QCD accuracy.

The photoproduction cross section  $d\Delta\sigma$  which is observed in experiment consists of two pieces: First, the *direct* part  $d\Delta\sigma_{\text{dir}}$ , where a quasi-real photon emitted from the lepton

beam scatters off parton  $b$  as an elementary particle such that  $a = \gamma$  in Eq. (1). Second, the *resolved* contribution  $d\Delta\sigma_{\text{res}}$ , where the photon resolves into “hadronic” constituents, which in turn interact with the partons emerging from the proton. In  $d\Delta\sigma_{\text{res}}$ ,  $a$  denotes the parton stemming from the photon. Direct and resolved contributions can be cast into the form of Eq. (1) by defining  $\Delta f_a^\ell$  as

$$\Delta f_a^\ell(x_a, \mu_f) = \int_{x_a}^1 \frac{dy}{y} \Delta P_{\gamma\ell}(y) \Delta f_a^\gamma \left( x_\gamma = \frac{x_a}{y}, \mu_f \right), \quad (2)$$

with

$$\begin{aligned} \Delta P_{\gamma\ell}(y) = & \frac{\alpha_e}{2\pi} \left\{ \left[ \frac{1 - (1-y)^2}{y} \right] \ln \frac{Q_{\text{max}}^2(1-y)}{m_\ell^2 y^2} \right. \\ & \left. + 2m_\ell^2 y^2 \left( \frac{1}{Q_{\text{max}}^2} - \frac{1-y}{m_\ell^2 y^2} \right) \right\} \end{aligned} \quad (3)$$

denoting the spin-dependent Weizsäcker-Williams “equivalent-photon” spectrum for the emission of a circularly polarized collinear photon with a virtuality smaller than  $Q_{\text{max}}^2$  by a lepton of mass  $m_\ell$  [9]. For the direct contribution,  $x_a$  has to be identified with the momentum fraction  $y$  of the lepton which is taken by the photon and thus

$$\Delta f_a^\gamma = \delta(1 - x_\gamma). \quad (4)$$

In the resolved case, the  $\Delta f_a^\gamma$  denote the parton distributions of the circularly polarized photon which are completely unmeasured so far.

It is important to note that beyond the leading order neither  $d\Delta\sigma_{\text{dir}}$  nor  $d\Delta\sigma_{\text{res}}$  are measurable cross sections *per se*, as their individual values depend on the factorization scheme chosen. Only if both pieces are evaluated using the same factorization prescription, their sum

$$d\Delta\sigma = d\Delta\sigma_{\text{dir}} + d\Delta\sigma_{\text{res}} \quad (5)$$

is a meaningful quantity. The unpolarized jet cross section,  $d\sigma = [d\sigma_{++} + d\sigma_{+-}]/2$ , is obtained in complete analogy to the polarized one by replacing all spin-dependent parton distributions and partonic cross sections with their spin-averaged counterparts. The spin-averaged equivalent-photon spectrum can be found in Ref. [15].

In order to compute the hard-scattering cross sections  $d(\Delta)\hat{\sigma}_{ab \rightarrow \text{jet}X}$ , an algorithm has to be specified describing the formation of jets by the partons which undergo the hard

scattering. A frequently adopted choice is to define a jet as the deposition of the total transverse energy of all final-state partons that fulfill

$$(\eta - \eta^i)^2 + (\phi - \phi^i)^2 \leq R^2, \quad (6)$$

where  $\eta^i$  and  $\phi^i$  denote the pseudo-rapidities and azimuthal angles of the particles and  $R$  the jet cone aperture. The jet variables are defined as

$$\begin{aligned} E_T &= \sum_i E_T^i, \\ \eta &= \sum_i \frac{E_T^i \eta^i}{E_T}, \\ \phi &= \sum_i \frac{E_T^i \phi^i}{E_T}. \end{aligned} \quad (7)$$

We resort to the so-called “small-cone approximation” [10], which can be considered as an expansion of the jet cross section in terms of  $R$  of the form  $\mathcal{A} \log R + \mathcal{B} + \mathcal{O}(R^2)$ . Neglecting  $\mathcal{O}(R^2)$  pieces, the evaluation and phase-space integration of the partonic cross sections can be performed analytically, as is our intention. The small-cone approximation has been shown [11, 12] to account extremely well for jet observables up to cone sizes of about  $R \approx 0.7$  by explicit comparison to calculations that take  $R$  fully into account. The predictions of Ref. [12] for single-inclusive jet production at the BNL-RHIC within the small-cone approximation are in excellent agreement with recent data from the STAR collaboration [16].

Since the resolved contribution  $d(\Delta)\sigma_{\text{res}}$  is technically equivalent to the jet production cross section in hadronic collisions,  $pp \rightarrow \text{jet}X$ , the corresponding partonic matrix elements squared can be taken from this previous calculation [12]. The direct contributions are adapted from the results for the  $d(\Delta)\hat{\sigma}_{\gamma b \rightarrow cX}$  in single-inclusive hadron photoproduction [17, 18] with the techniques of Ref. [12].

The hard-scattering cross sections are then implemented in a Monte-Carlo program which performs the convolutions with the parton distributions of the proton and with the equivalent photon spectrum numerically by means of an adaptive VEGAS integration.

As consistency check, we have calculated jet cross sections for HERA kinematics and compared our results successfully to those of Refs. [6, 8, 9].

### III. NUMERICAL RESULTS

We now turn to a phenomenological study of jet production at future lepton-hadron colliders. Our aim is twofold: First, we will discuss the impact of NLO corrections on transverse momentum and rapidity distributions in various kinematic regimes and explore the stability of our predictions with respect to scale variations. Second, we will investigate the sensitivity of jet-production cross sections to the parton distribution functions of the photon and the proton and demonstrate how to increase the impact of specific contributions by adjusting parameters of the analysis.

#### A. Single-inclusive jet production at the LHeC

New opportunities for the measurement of single-inclusive jets in lepton-hadron collisions could be provided by a future LHeC  $ep$  collider at CERN, which is currently under scrutiny [14]. In the following we will present predictions for the scenario where an electron beam circulates in the existing LHC tunnel with a nominal energy of  $E_e = 70$  GeV, which in conjunction with the 7 TeV proton beam gives rise to  $ep$  collisions with a c.m.s. energy of  $\sqrt{S} = 1.4$  TeV.

For the equivalent-photon approximation [15] similar parameters as for the H1 and ZEUS experiments at HERA are used,  $Q_{\max}^2 = 1$  GeV<sup>2</sup> and  $0.2 \leq y \leq 0.85$ . All LO (NLO) calculations are performed with the CTEQ6L (CTEQ6M) parton distributions [19] and the according one-loop (two-loop) values for the strong coupling constant  $\alpha_s$  in the  $\overline{\text{MS}}$ -factorization scheme. For the parton distribution functions of the photon the LO (NLO) GRV set [20] is employed.

The major motivation for studying jet cross sections beyond leading order is to reduce the theoretical uncertainties associated with a tree-level calculation. To access the improvement which can be gained by the inclusion of NLO corrections the single-inclusive jet cross section at the LHeC is shown in Fig. 1 as function of the jet transverse momentum  $p_T$  at LO and NLO. The jet cone size is set to  $R = 0.7$  and rapidities are integrated over  $-1 < \eta < 4$  in the laboratory frame. The solid lines correspond to the setting  $\mu_r = \mu_f = p_T$ . The bands have been obtained by varying the factorization and renormalization scales simultaneously in the range  $p_T/2 \leq \mu_r = \mu_f \leq 2p_T$ . Throughout the  $p_T$  interval considered, the scale dependence

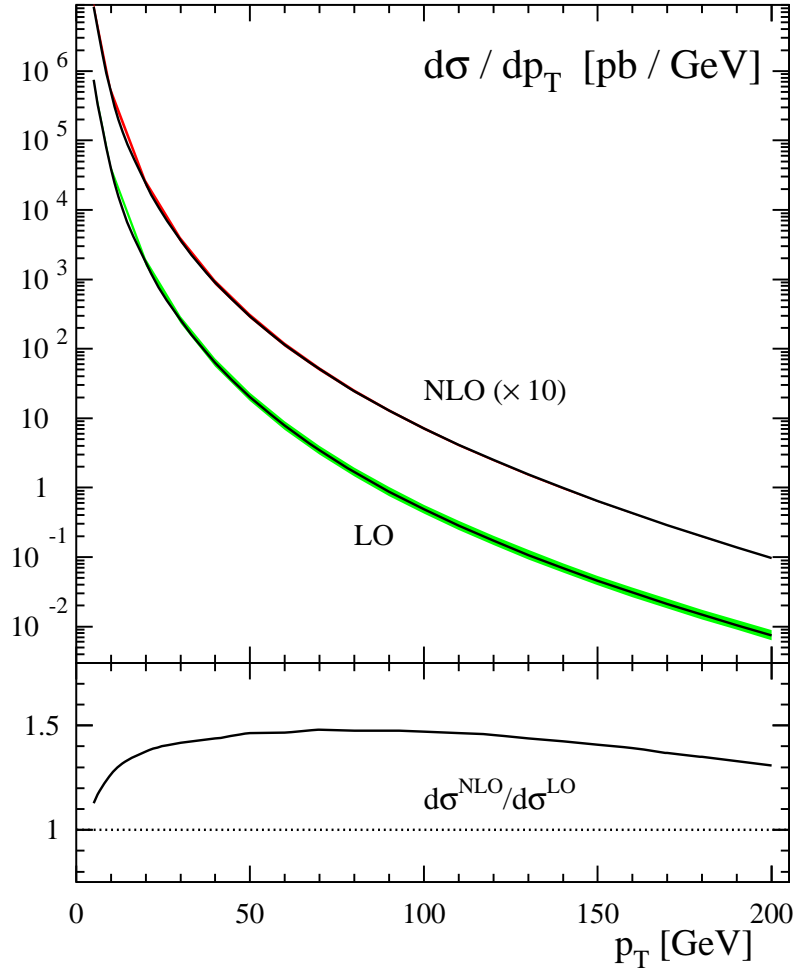


FIG. 1: Single-inclusive jet cross section at the LHeC as function of  $p_T$  in NLO (multiplied by a factor of 10) and LO, integrated over  $-1 < \eta < 4$ . The shaded bands correspond to a scale variation of the NLO and LO results, respectively, in the range  $p_T/2 \leq \mu_r = \mu_f \leq 2p_T$ . The lower panel shows the associated K factor.

is very small at LO already, amounting to about  $20 \div 30$  %. While at low values of  $p_T$  the NLO corrections do not significantly improve the scale dependence of the cross section, towards higher  $p_T$  the scale uncertainty of the NLO result is extremely small, going down to the level of 2.5 % at  $p_T = 200$  GeV. This behavior indicates that the perturbative expansion is under excellent control, provided single-inclusive jets are produced at high transverse momentum. The impact of the NLO corrections on the cross section is indicated by the

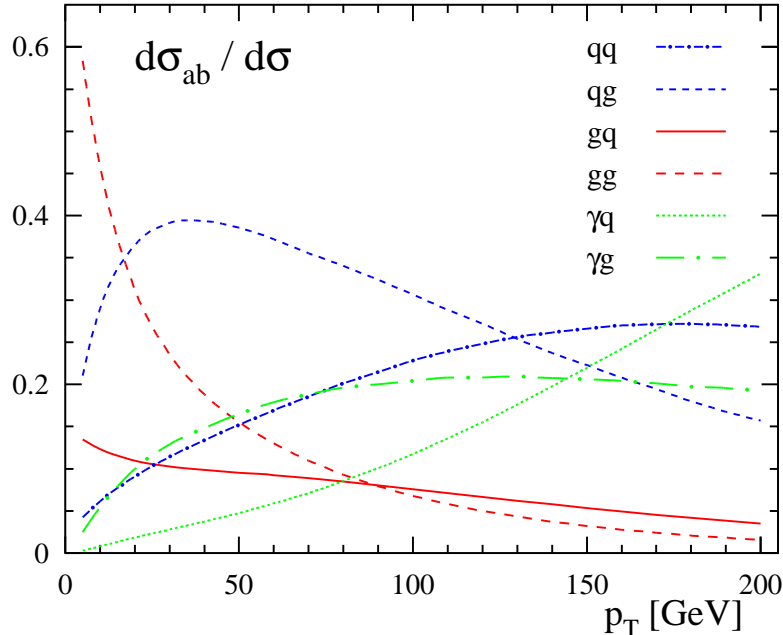


FIG. 2: Relative contributions of different partonic subprocesses  $ab \rightarrow \text{jet}X$  to the NLO single-inclusive jet cross section at the LHeC, integrated over  $-1 < \eta < 4$ .

K factor, which we define as

$$K(x) = \frac{d\sigma^{\text{NLO}}/dx}{d\sigma^{\text{LO}}/dx}. \quad (8)$$

For  $\mu_r = \mu_f = p_T$ ,  $K(p_T)$  is larger than one everywhere, which reflects the increase of the cross section by the inclusion of the NLO contributions.

Figure 2 illustrates the contributions of different partonic subprocesses to the rapidity-integrated NLO cross section. The resolved contributions are dominant over a large range of  $p_T$  with the direct contributions starting to take over only at  $p_T \approx 200$  GeV. Since the cross section is largest at low values of  $p_T$ , this indicates that single-inclusive jet production at LHeC energies offers excellent opportunities for a more accurate determination of the parton content of the photon.

To this end, the study of rapidity-differential cross sections is particularly suitable, since the momentum fractions of the hadronic constituents of the photon and the proton can be considered as functions of the rapidity of the observed jet in the laboratory frame,  $\eta$ . As explained, e.g., in Ref. [8], if counting positive rapidity in the forward direction of the proton,

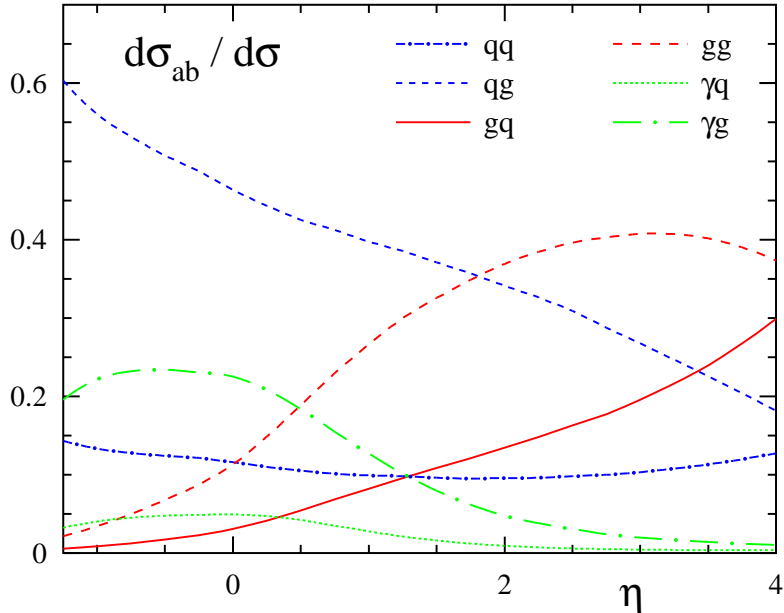


FIG. 3: Relative contributions of different partonic subprocesses  $ab \rightarrow \text{jet}X$  to the NLO single-inclusive jet cross section at the LHeC, integrated over  $p_T > 20$  GeV.

large  $x_\gamma \rightarrow 1$  are probed at large negative values of  $\eta$ . In this region, the direct contribution is expected to be largest and the  $f^\gamma$  are dominated by the purely perturbative “pointlike” part which does not depend on the hadronic structure of the photon. The relative contributions of the various direct and resolved channels to the full cross section are depicted as function of rapidity in Fig. 3.

The LO and NLO rapidity-dependent jet cross sections integrated over  $p_T > 20$  GeV are shown in Fig. 4 along with the associated scale uncertainties, obtained by varying renormalization and factorization scales simultaneously in the range  $p_T/2 \leq \mu_r = \mu_f \leq 2p_T$ . Also shown are the relative contributions of the direct and the resolved cross sections at NLO. Strikingly, the scale uncertainty of the rapidity distribution is not improved by the inclusion of NLO corrections. This feature can be traced back to the large weight of contributions from relatively low  $p_T$ , where the LO and the NLO scale dependences are of similar size, c.f. Fig. 1. After imposing a transverse momentum cut of  $p_T > 40$  GeV, the scale dependence is slightly improved with the size of the cross section being reduced at the same time by approximately one order of magnitude. Even smaller scale uncertainties are obtained for

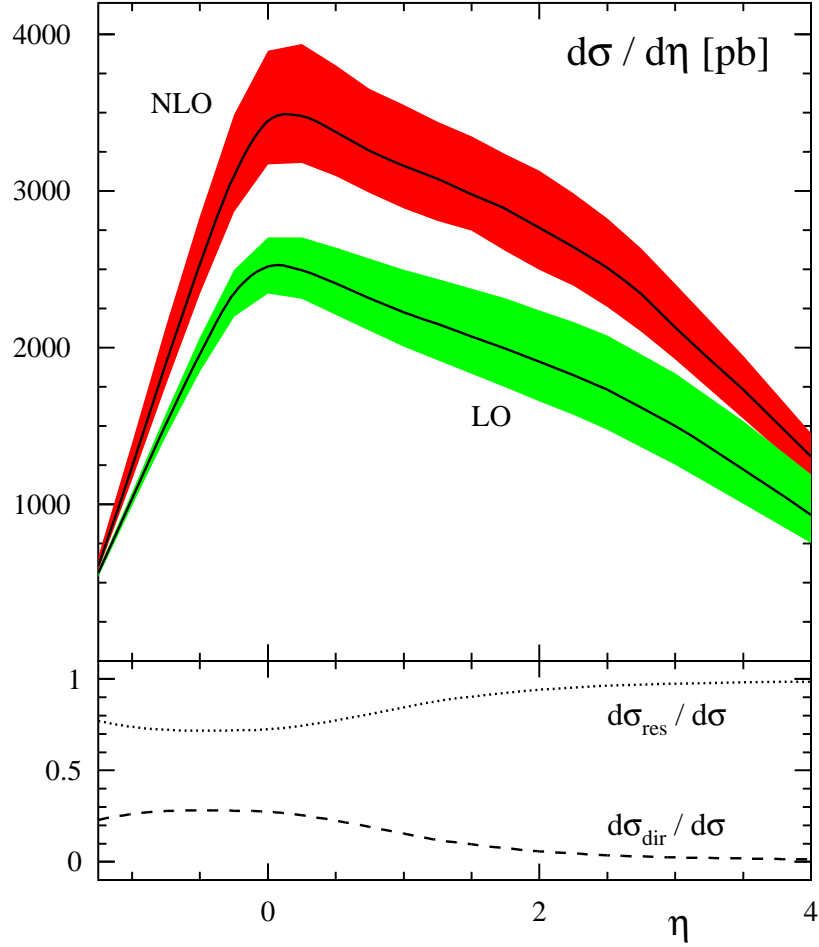


FIG. 4: Single-inclusive jet cross section at the LHeC as function of  $\eta$  in NLO and LO, integrated over  $p_T > 20$  GeV. The shaded bands correspond to a scale variation in the range  $p_T/2 \leq \mu_r = \mu_f \leq 2p_T$ . The lower panel depicts the relative contributions of the direct and resolved sub-processes to the NLO cross section.

$p_T > 100$  GeV, see Fig. 5. As the transverse momentum cut is increased, the impact of the direct photon contributions becomes larger and the resolved sub-processes start to be less important.

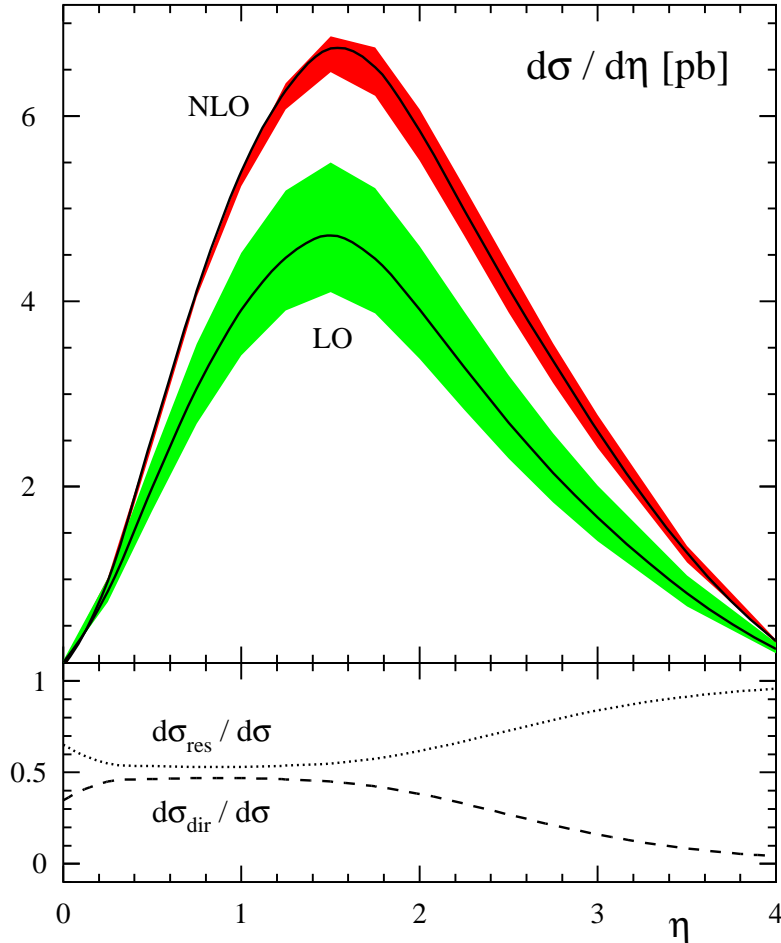


FIG. 5: Same as in Fig. 4, but now integrated over  $p_T > 100$  GeV.

### B. Polarized photoproduction of single-inclusive jets at eRHIC

Photoproduction experiments complimentary to the measurements possible at the LHeC could be performed at the future lepton-proton collider eRHIC at BNL [13]. The polarized beams available at eRHIC offer unique opportunities for studying the spin structure of the circularly polarized photon, which is completely unknown so far.

In the following we assume a hadronic c.m.s. energy of  $\sqrt{S} = 100$  GeV. For the equivalent-photon approximation [9, 15] we choose  $Q_{\max}^2 = 1$  GeV<sup>2</sup> and  $0.2 \leq y \leq 0.85$ . In the unpolarized case, we stick to the parton distributions of Sec. III A. For the spin-dependent proton distribution functions we use the GRSV standard set [21] as default, since it contains

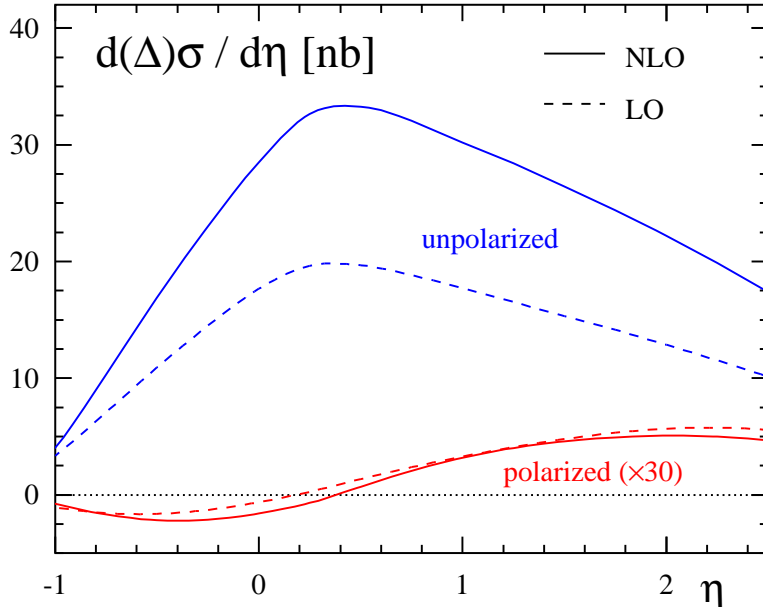


FIG. 6: Polarized and unpolarized single-inclusive jet cross sections at eRHIC as function of  $\eta$  in NLO and LO, integrated over  $p_T > 4$  GeV. The polarized cross section is multiplied by a factor of 30.

both, a LO and an NLO parameterization. To illustrate the impact of different parton densities, we will also employ the new DSSV set [3], which is only available at NLO, however. The parton distributions of the polarized photon are completely unmeasured so far. We therefore consider the two extreme scenarios of Ref. [22] with minimal [ $\Delta f^\gamma(x, \mu_0) = 0$ ] and maximal [ $\Delta f^\gamma(x, \mu_0) = f^\gamma(x, \mu_0)$ ] saturation of the positivity constraint  $|\Delta f^\gamma(x, \mu_0)| \leq f^\gamma(x, \mu_0)$  [23]. Here,  $\mu_0$  denotes the scale where the boundary conditions for the evolution are fixed. If not specified otherwise, the “maximal” set will be used.

Figure 6 shows the rapidity dependent unpolarized and polarized single-inclusive jet cross sections at LO and NLO integrated over  $p_T > 4$  GeV. The spin-averaged cross section receives sizeable positive NLO corrections resulting in  $1.2 \lesssim K(\eta) \lesssim 1.7$ . In the spin-dependent case, the NLO effects are rather small yielding a K factor close to one over a large range in  $\eta$ .

The scale uncertainty of the polarized cross section, illustrated by Fig. 7, is sizably reduced at NLO. Scale dependences are generally smaller for jet cross sections than for

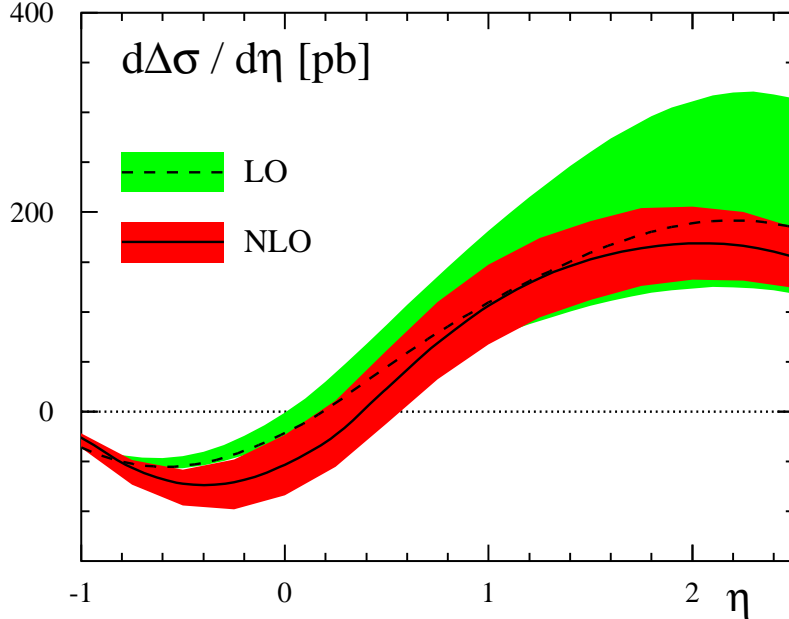


FIG. 7: Single- inclusive jet cross section at eRHIC as function of  $\eta$  in NLO and LO, integrated over  $p_T > 4$  GeV. The shaded bands correspond to a scale variation in the range  $p_T/2 \leq \mu_r = \mu_f \leq 2p_T$ .

related hadron-production observables, such as the pion-production cross sections at eRHIC discussed in Ref. [17]. This hierarchy is also observed in related  $pp$ -scattering reactions (see Refs. [12, 24]) and is mainly due to the presence of scale dependent fragmentation functions in processes with identified hadrons. These non-perturbative objects describe the formation of hadrons from the final-state partons in a hard-scattering process at a specific scale, which may be different from the scale at which initial-state singularities are factorized into the distribution functions of the photon and proton, respectively.

For extracting information on the hadronic structure of the circularly polarized photon the experimentally accessible spin asymmetry

$$A_{LL}^{\text{jet}} = \frac{d\Delta\sigma}{d\sigma} = \frac{d\sigma_{++} - d\sigma_{+-}}{d\sigma_{++} + d\sigma_{+-}} \quad (9)$$

is most suitable. At large positive rapidities,  $A_{LL}^{\text{jet}}$  is particularly sensitive to the parton content of the resolved photon as exemplified in Fig. 8, where the spin asymmetry is shown for the two extreme sets of polarized photon densities introduced above. To demonstrate that this sensitivity is not obscured by our currently incomplete knowledge of the polarized

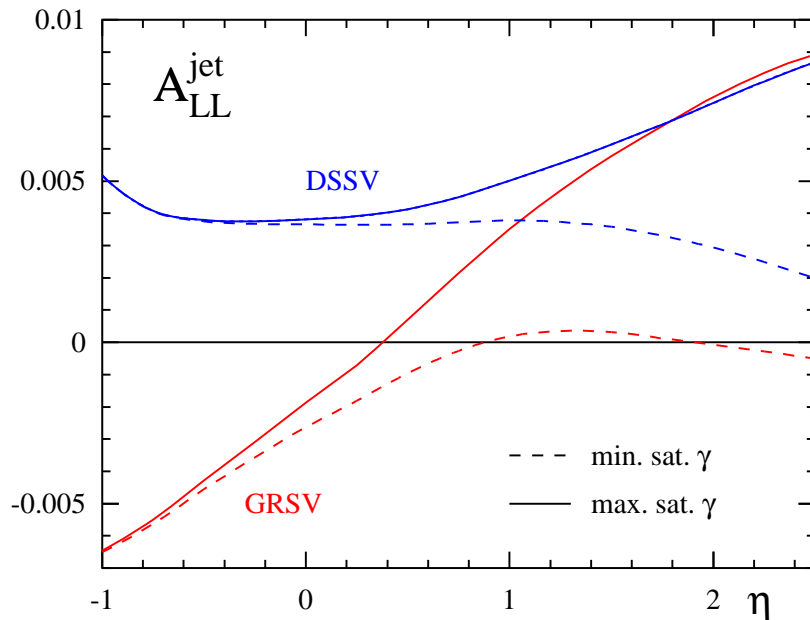


FIG. 8: NLO-QCD spin asymmetry for single-inclusive jet photoproduction at eRHIC integrated over  $p_T > 4$  GeV for two different choices of proton distribution functions and the two extreme sets of polarized photon densities.

proton, predictions are made for two different sets of proton distributions which mainly differ in the parameterization of the polarized gluon density. Towards negative values of  $\eta$ ,  $A_{LL}^{\text{jet}}$  becomes less sensitive to the hadronic structure of the photon. With the  $qg$  subprocess being dominant in this region, the spin asymmetry could provide new information on the gluon density of the proton.

#### IV. CONCLUSIONS

In this work an NLO-QCD calculation of single-inclusive jet photoproduction in unpolarized and longitudinally polarized lepton-hadron collisions has been presented. The computation was performed in the context of the small-cone approximation. In this way, the evaluation of the partonic matrix elements and large parts of the phase-space integration could be performed analytically, yielding a stable and much faster computer code than comparable programs that are based on a purely numerical approach.

We have performed a phenomenological analysis of jet photoproduction at future  $ep$  colliders, in particular the LHeC and eRHIC. We found that NLO corrections are sizeable at the LHeC with K factors of about 1.5. In the low-to-moderate  $p_T$  regime the resolved photon contributions are by far dominant and scale uncertainties are large even beyond the leading order. If a large transverse momentum cut is imposed, these uncertainties can be brought down. At high  $p_T$ , quark-initiated processes dominate over the gluonic channels.

For eRHIC, we have focused on jet photoproduction by longitudinally polarized beams. Polarized cross sections exhibit smaller NLO corrections than their spin-averaged counterparts with K factors close to one and only moderate scale dependences. The experimentally relevant double-spin asymmetry exhibits pronounced sensitivity to the hadronic structure of the (resolved) photon in the positive-rapidity regime. At negative values of  $\eta$ ,  $A_{LL}^{\text{jet}}$  could yield further information on the gluon polarization of the proton complementary to experiments in hadron-hadron collisions.

In summary, future lepton-hadron colliders offer new possibilities for further constraining the hadronic structure of the (real) photon in the unpolarized case, and unique opportunities to access the completely unknown parton distributions of the polarized photon. Embedded in a global analysis of hadronic scattering reactions, single-inclusive jet production will also help to further pin down the parton densities of the proton, in particular its gluonic component.

## Acknowledgments

I am grateful to Marco Stratmann for valuable discussions and comments. This work was supported by the Japan Society for the Promotion of Science (JSPS).

- 
- [1] P. Nadolsky et al., arXiv: 0802.0007 [hep-ph].
  - [2] A. D. Martin, W. J. Stirling, R. S. Thorne, and G. Watt, Phys. Lett. B **652**, 292 (2007).
  - [3] D. de Florian, R. Sassot, M. Stratmann, and W. Vogelsang, arXiv: 0804.0422 [hep-ph].
  - [4] for a recent review see, e.g.: M. Klein and R. Yoshida, arXiv: 0805.3334 [hep-ex].
  - [5] L. E. Gordon and J. K. Storrow, Phys. Lett. B **291**, 320 (1992);  
D. Bödeker, Phys. Lett. B **292**, 164 (1992); Z. Phys. C **59**, 501 (1993);

- G. Kramer and S. G. Salesch, *Z. Phys. C* **61**, 277 (1994);
- D. Bödeker, G. Kramer, and S. G. Salesch, *Z. Phys. C* **63**, 471 (1994);
- S. Frixione, *Nucl. Phys. B* **507**, 295 (1997);
- S. Frixione and G. Ridolfi, *Nucl. Phys. B* **507**, 315 (1997).
- [6] B. W. Harris and J. F. Owens, *Phys. Rev. D* **56**, 4007 (1997).
- [7] See, e.g., *Proceedings of the Workshop “Physics with Polarized Protons at HERA”, Hamburg, Germany, 1997*, edited by A. De Roeck and T. Gehrmann, DESY-PROC-1998-01.
- [8] M. Stratmann and W. Vogelsang, *Z. Phys. C* **74**, 641 (1997);
- M. Stratmann and W. Vogelsang, in *Proceedings of the Workshop “Future Physics at HERA”, Hamburg, Germany, 1995/96*, edited by G. Ingelman, A. de Roeck, and R. Klanner, p. 815;
- J.M. Butterworth, N. Goodman, M. Stratmann, and W. Vogelsang, in *Proceedings of the Workshop “Physics with Polarized Protons at HERA”, Hamburg, Germany, 1997*, arXiv: hep-ph/9711250.
- [9] D. de Florian and S. Frixione, *Phys. Lett. B* **457**, 236 (1999).
- [10] G. Sterman and S. Weinberg, *Phys. Rev. Lett.* **39**, 1436 (1977);
- M.A. Furman, *Nucl. Phys. B* **197**, 413 (1982);
- F. Aversa, P. Chiappetta, M. Greco, and J.-Ph. Guillet, *Nucl. Phys. B* **327**, 105 (1989);
- Z. Phys. C* **46**, 253 (1990).
- [11] F. Aversa, P. Chiappetta, M. Greco, and J.-Ph. Guillet, *Phys. Rev. Lett.* **65**, 401 (1990);
- F. Aversa et al., *Z. Phys. C* **49**, 459 (1991);
- J.-Ph. Guillet, *Z. Phys. C* **51**, 587 (1991).
- [12] B. Jäger, M. Stratmann, and W. Vogelsang, *Phys. Rev. D* **70**, 034010 (2004).
- [13] See <http://www.bnl.gov/eic> for information concerning the eRHIC/EIC project, including the Whitepaper BNL-68933.
- [14] J. B. Dainton et al., *JINST* **1**, P10001 (2006).
- [15] S. Frixione, M. L. Mangano, P. Nason, and G. Ridolfi, *Phys. Lett. B* **319**, 339 (1993).
- [16] STAR Collaboration, B. I. Abelev et al., *Phys. Rev. Lett.* **97**, 252001 (2006).
- [17] B. Jäger, M. Stratmann, and W. Vogelsang, *Phys. Rev. D* **68**, 114018 (2003).
- [18] B. Jäger, M. Stratmann, and W. Vogelsang, *Eur. Phys. J. C* **44**, 533 (2005).
- [19] J. Pumplin et al., *JHEP* **07**, 012 (2002).
- [20] M. Glück, E. Reya, and A. Vogt, *Phys. Rev. D* **46**, 1973 (1992).

- [21] M. Glück, E. Reya, M. Stratmann, and W. Vogelsang, Phys. Rev. D **63**, 094005 (2001).
- [22] M. Stratmann and W. Vogelsang, Phys. Lett. B **386**, 370 (1996).
- [23] M. Glück and W. Vogelsang, Z. Phys. C **55**, 353 (1992); *ibid.* **C57**, 309 (1993);  
M. Glück, M. Stratmann, and W. Vogelsang, Phys. Lett. B**337**, 373 (1994).
- [24] B. Jäger, A. Schäfer, M. Stratmann, and W. Vogelsang, Phys. Rev. D **67**, 054005 (2003).